Optimisation of switching frequency of three-phase four-wire inverter under different dead time

Fuzhuan Wu, Mengna Chen, Sheng Peng and Shengjun Wen*

Department of Electric and Information Engineering,
Zhongyuan University of Technology,
No. 41 Zhongyuan Road, Zhengzhou, Henan Province, 450007, China
Email: wfzh@zut.edu.cn
Email: cmn0828@163.com
Email: 9907@zut.edu.cn
Email: wsj@zut.edu.cn
*Corresponding author

Abstract: Aiming at the selection of inverter switching frequency and the harmonic problem of the dead time in reality, an optimal method for switching frequency of three-phase four-wire inverters considering the dead time to reduce the total harmonic distortion (THD) was proposed. Firstly, the output sinusoidal pulse width modulation (SPWM) wave was analysed by using double Fourier transform and Bessel function, and the spectrum of SPWM with dead time was obtained. Secondly, the relationship between the THD of the output voltage and the switching frequency was analysed. The study found that there is an optimal switching frequency to minimise the output voltage THD. Thirdly, the linear Lagrangian interpolation method was used to fit the formula for selecting the optimal switching frequency with different dead time. Finally, a three-phase four-wire inverter test prototype based on the TMS320F28335 control chip was built, and the effectiveness of the proposed method was verified through experiments.

Keywords: switching frequency; dead time; three-phase four-wire inverter; total harmonic distortion; THD.

Reference to this paper should be made as follows: Wu, F., Chen, M., Peng, S. and Wen, S. (2022) 'Optimisation of switching frequency of three-phase four-wire inverter under different dead time', *Int. J. Advanced Mechatronic Systems*, Vol. 9, No. 4, pp.219–226.

Biographical notes: Fuzhuan Wu is a Professor at Zhongyuan University of Technology. He received his BS from Harbin University of Science and Technology, China, in 1988. He has been a Professor at Zhongyuan University of Technology, since 2011. His interest fields include power electronics and power drives, power quality conditioner.

Mengna Chen is a Master student at Zhongyuan University of Technology, China. She received her BS from Huanghuai University, China, in 2018. Her interest fields include electrical control and smart grid.

Sheng Peng is a Bachelor student at Zhongyuan University of Technology, China, in 2006. He has been an experimentalist at Zhongyuan University of Technology since 2012. His interest fields include power electronics and power drives, power quality conditioner.

Shengjun Wen is a Professor at Zhongyuan University of Technology. In 2011, he obtained his PhD in Electronic and Information Engineering from Graduate School of Engineering in Tokyo University of Agriculture and Technology. He earned his BS and MS in Electrical Engineering from Zhengzhou University, China, in 2001 and 2004 respectively. His interest fields include nonlinear control, adaptive control, fault diagnosis and robotics.

1 Introduction

Power generation and distribution technology based on renewable energy has developed rapidly, due to global warming and limited fossil energy (Song et al., 2011; Emami and Banazadeh, 2013). Inverters play a role as a link among them. SPWM inverters were widely used due to their simple structure and fast dynamic response (Ma et al., 2020). However, the harmonic problem also exists with the high-speed switching of the switch tube. The total harmonic distortion (THD) of the voltage output by the inverter is one of the important indicators to measure its performance. The selection of switching frequency is closely related to THD. Therefore, the determination of switching frequency is very

necessary in the parameter design of the inverter (Zhang et al., 2018).

In fact, the switching tube cannot be turned on and off in an instant, due to the existence of the switching tube junction capacitance. Therefore, the dead time needs to be set to avoid the state where the upper and lower switch tubes are simultaneously conducting (Huang et al., 2018). Because of the dead time, the ability of the system to output voltage is reduced, causing harmonic problems such as phase deviation and waveform distortion in the voltage waveform (Song et al., 2014; Jeong et al., 1991).

Aiming at the harmonic problem of SPWM inverter, Holmes (1998) conducted a detailed analysis of the ideal SPWM wave, which provided an important basis for the follow-up research. In view of the optimisation of the output power quality of the inverter considering the dead time, many experts and scholars (Sukegawa et al., 1988; Ni et al., 2019; Wang et al., 2020) proposed methods of dead time compensation. This will increase a certain degree of software or hardware complexity. Researchers (Wu et al., 2001) showed that a reasonable increase in the switching frequency can prevent harmonic generation, but did not provide an appropriate method. Researchers Sun et al. (2020) and Hu et al. (2015) respectively use rotor loss and efficiency as standards to provide a reference for the selection of switching frequency.

This paper takes the three-phase four-wire inverter as the research object. Based on the harmonic analysis of the inverter containing the dead time, the relationship between the output voltage THD and the switching frequency was studied in detail. A method of optimising the switching frequency was proposed.

2 Harmonic analysis

2.1 SPWM harmonic analysis under ideal conditions

Figure 1 shows the topology of a the three-phase four-wire SPWM inverter. The reference direction of voltage V_{in} and current i is shown in Figure 1.

The three-phase modulation waves u_U, u_V, u_W and carrier u_c can be expressed as:

$$\begin{cases} u_U = U_s \sin(\omega_s t + \varphi) \\ u_V = U_s \sin(\omega_s t + \varphi - 2\pi/3) \\ u_W = U_s \sin(\omega_s t + \varphi + 2\pi/3) \end{cases} \tag{1}$$

$$u_c = \begin{cases} \left(\omega_c t - 2k\pi + \dfrac{\pi}{2}\right)\dfrac{2U_c}{\pi} - U_c \\ \omega_c t \in [(2k-1)\pi, 2k\pi] \\ -\left(\omega_c t - 2k\pi - \dfrac{\pi}{2}\right)\dfrac{2U_c}{\pi} + U_c \\ \omega_c t \in [2k\pi, (2k+1)\pi] \end{cases} \tag{2}$$

In the formula, k = 0, 1, 2, 3, ….

Figure 1 The three-phase four-wire SPWM inverter topology diagram

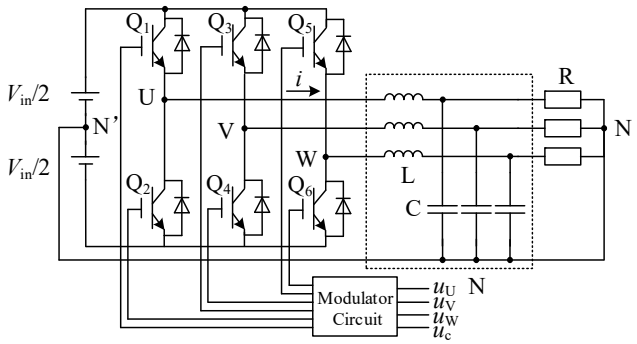

Ideally, there are few low-order harmonics in the output SPWM. And it only contains harmonics which are multiples of the switching angle frequency and its vicinity, such as ω_c, $2\omega_c$, and $3\omega_c$. The amplitude of the harmonic component at the switching angle frequency ω_c is the highest.

The LC filter shown in Figure 1 was used in this paper, and the current ripple is usually selected as 20% (Chitsazan and Trzynadlowski, 2017). The design formulas for the filter inductance L and capacitance C are as follows:

$$L = \frac{V_{in}}{8 \times f_c \times 20\% \times I_o} \tag{3}$$

$$C = \left(\frac{10}{2\pi f_c}\right)^2 \frac{1}{L} \tag{4}$$

In the formula:

V_{in} DC side voltage

I_o at rated output current, the fundamental wave effective value of the inductor current on the inverter side

f_c switching frequency.

2.2 SPWM harmonic analysis considering dead time

To prevent the upper and lower insulated gate bipolar transistors (IGBTs) of the same bridge arm from being turned on at the same time, it is often requisite to set a dead time. Therefore, it is necessary to perform harmonic analysis on the output SPWM voltage when the dead time is considered.

Figure 2 is a schematic diagram of SPWM wave generation when the dead time is considered. The dead time setting can be equivalent to the ideal SPWM wave superimposing a series of dead time pulses. When setting the dead time, the actual output PWM wave is different from the ideal SPWM wave by a dead time pulse with a width of Δt at the initial position of each switching cycle. And the polarity of the dead time pulse is opposite to the SPWM wave. It is not difficult to obtain that the frequency of $u_{\Delta t}$ is the same as the frequency of the modulating wave, and the dead time pulses of the positive and the negative half-waves are symmetrical.

Figure 2 Schematic diagram of SPWM waves generated when dead time is considered

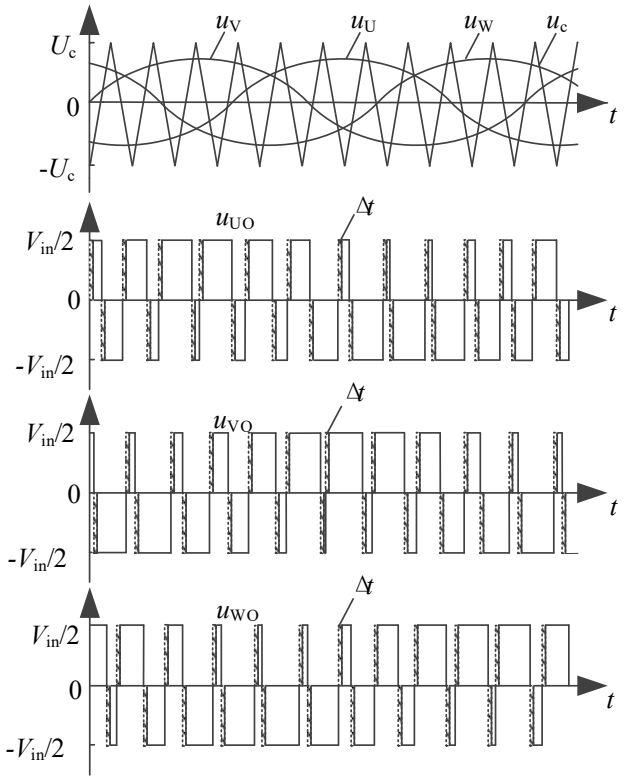

The influence of the dead time pulse on the fundamental voltage amplitude can be expressed as $u_{\Delta t}$:

$$u_{\Delta t} = Nf_s\Delta tV_{in} = f_c\Delta tV_{in} \tag{5}$$

In the formula:

N carrier ratio

f_s modulating wave frequency

Δt dead time.

For a three-phase four-wire inverter, when the U, V, and W terminals are unloaded or connected to a pure resistive load, the diode has no freewheeling current. Suppose the initial phase of u_{UN} is zero, the phase of u_{VN} is later than the phase of u_{UN} by $2\pi/3$, and the phase of u_{WN} is ahead of the phase of u_{UN} by $2\pi/3$. According to the bilateral Fourier transform and Bessel function, the Fourier series expansion of the output voltage u_{UN}, u_{VN} and u_{WN} can be deduced as:

$$\begin{aligned}
u_{UN}(t) &= \frac{M_r V_{in}}{2}\sin\omega_s t \\
&+\frac{2V_{in}}{\pi}\sum_{m=1,3,5,\cdots}^{\infty}\sum_{n=0,\pm2,\pm4,\cdots}^{\pm\infty}\frac{J_n(mM_r\pi/2)}{m}\sin\left(\frac{m\Delta t\omega_c}{2}\right)\cos\left(m\omega_c t\right. \\
&\left.+n\omega_s t-\frac{m\Delta t\omega_c}{2}\right) \\
&+\frac{2V_{in}}{\pi}\sum_{m=2,4,6,\cdots}^{\infty}\sum_{n=\pm1,\pm3,\cdots}^{\pm\infty}\frac{J_n(mM_r\pi/2)}{m}\cos\left(\frac{m\Delta t\omega_c}{2}\right)\sin\left(m\omega_c t\right. \\
&\left.+n\omega_s t-\frac{m\Delta t\omega_c}{2}\right)
\end{aligned} \tag{6}$$

$$\begin{aligned}
u_{VN}(t) &= \frac{M_r V_{in}}{2}\sin\left(\omega_s t-\frac{2\pi}{3}\right) \\
&+\frac{2V_{in}}{\pi}\sum_{m=1,3,5,\cdots}^{\infty}\sum_{n=0,\pm2,\pm4,\cdots}^{\pm\infty}\frac{J_n(mM_r\pi/2)}{m}\sin\left(\frac{m\Delta t\omega_c}{2}\right)\cos\left[m\omega_c t\right. \\
&\left.+n\left(\omega_s t-\frac{2\pi}{3}\right)-\frac{m\Delta t\omega_c}{2}\right] \\
&+\frac{2V_{in}}{\pi}\sum_{m=2,4,6,\cdots}^{\infty}\sum_{n=\pm1,\pm3,\cdots}^{\pm\infty}\frac{J_n(mM_r\pi/2)}{m}\cos\left(\frac{m\Delta t\omega_c}{2}\right)\sin\left[m\omega_c t\right. \\
&\left.+n\left(\omega_s t-\frac{2\pi}{3}\right)-\frac{m\Delta t\omega_c}{2}\right]
\end{aligned} \tag{7}$$

$$\begin{aligned}
u_{WN}(t) &= \frac{M_r V_{in}}{2}\sin\left(\omega_s t+\frac{2\pi}{3}\right) \\
&+\frac{2V_{in}}{\pi}\sum_{m=1,3,5,\cdots}^{\infty}\sum_{n=0,\pm2,\pm4,\cdots}^{\pm\infty}\frac{J_n(mM_r\pi/2)}{m}\sin\left(\frac{m\Delta t\omega_c}{2}\right)\cos\left[m\omega_c t\right. \\
&\left.+n\left(\omega_s t+\frac{2\pi}{3}\right)-\frac{m\Delta t\omega_c}{2}\right] \\
&+\frac{2V_{in}}{\pi}\sum_{m=2,4,6,\cdots}^{\infty}\sum_{n=\pm1,\pm3,\cdots}^{\pm\infty}\frac{J_n(mM_r\pi/2)}{m}\cos\left(\frac{m\Delta t\omega_c}{2}\right)\sin\left[m\omega_c t\right. \\
&\left.+n\left(\omega_s t+\frac{2\pi}{3}\right)-\frac{m\Delta t\omega_c}{2}\right]
\end{aligned} \tag{8}$$

Among them:

M_r modulation ratio

$J_n(x)$ Bessel function.

The definition of voltage THD rate is as follows (Zhou et al., 2010):

$$THD = \sqrt{\sum_{n=2}^{H}\left(\frac{V_n}{V_1}\right)^2} = \sqrt{\frac{\sum_{n=2}^{H}V_n^2}{V_1^2}} \tag{9}$$

where V_n is the harmonic component voltage, V_1 is the fundamental component voltage.

For the convenience of calculation, an approximate method is used here for analysis. The THD is approximately expressed as the relationship between the dead time pulse's influence on the fundamental voltage amplitude $u_{\Delta t}$ and the fundamental effective value U:

$$THD \approx \frac{u_{\Delta t}}{u_{\Delta t}+U} \approx \frac{u_{\Delta t}}{U} \tag{10}$$

The effective value of the fundamental voltage can be expressed as:

$$U = \frac{M_r \times V_{in}}{\sqrt{2}} \tag{11}$$

In engineering, THD is usually required to be less than 5%. Substituting formula (5) and formula (11) into formula (10), the range of switching frequency f_c can be obtained. However, this method cannot determine the optimal switching frequency. Therefore, we use MATLAB Simulink FFT tool for spectrum analysis. The spectrum diagram of

SPWM wave u_{uv} when dead time was considered is shown in Figure 3.

Figure 3 The spectrum diagram of PWM wave u_{uv} when dead time is considered (see online version for colours)

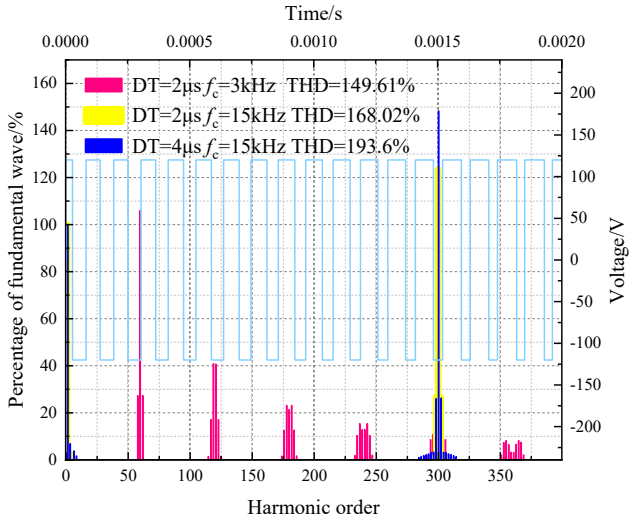

In the figure, the light blue line is the waveform of u_{uv} the red bar is the spectrum with the dead time of 2 μs and the switching frequency of 3 kHz, the yellow bar is the spectrum with the dead time of 2 μs and the switching frequency of 15 kHz, and the navy blue bar is the spectrum with the dead time of 4 μs and the switching frequency of 15 kHz.

It is not difficult to see that the harmonic distribution considering the dead time becomes complicated, and there is a small amount of low-order harmonics. Harmonics are mainly concentrated in the vicinity of the switching frequency and the integer multiples of the frequency. The THD of u_{uv} increases with the increase of dead time and switching frequency. There are two main reasons for the above situation:

1 When Δt is wider than the SPWM pulse near the zero crossing, these pulses will be lost. This will distort the waveform near the zero-crossing point and increases the THD.

2 The dead time pulse has the same frequency and opposite polarity as the fundamental wave, which causes the fundamental wave amplitude to drop. Especially, the fundamental wave amplitude will drop more obviously when the dead time pulse is wider.

When the dead time is fixed, increasing the switching frequency will result in a further increase in the content of low-order harmonics and a further increase in THD. When the switching frequency is constant, the increase of the dead time will lead to the increase of the low-order harmonic content and THD.

To further study the relationship between THD, switching frequency and dead time of the inverter output voltage, the LC filter designed by formula (3) and formula (4) was adopted. The relationship between the THD of the filtered output voltage and the switching frequency f_c is shown in Figure 4.

Figure 4 The relationship between THD and switching frequency (see online version for colours)

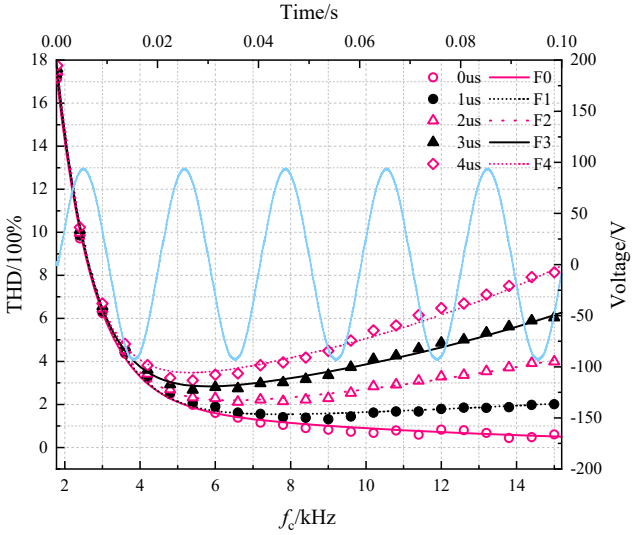

In the figure, the light blue line is the sine waveform of SPWM filtered by LC filter, and the scatter plot is the trend of THD changing with the switching frequency. Since the selection of simulation data points is discrete, it is inevitable that there will be slight fluctuations. In the project, in order to facilitate the analysis, the fitting process is performed, and the fitting curve obtained is shown in Figure 4.

It can be seen from the figure that when the dead time is 0 μs, the THD of output voltage gradually decreases with the increase of f_c. When the dead time is greater than 0 μs, the THD first decreases to the minimum and then gradually increases with the increase of f_c. And the longer the dead time, the more obvious the trend. This is different from the changing trend of THD when the dead time is 0 μs. Its biggest feature is that there is a switching frequency that minimises THD.

3 Dead time setting

3.1 Dead time calculation

Considering the actual situation, the setting of the dead time depends on the working process of the IGBT. Infineon uses the method shown in Figure 5 to define the switching time of the IGBT.

To prevent the upper and lower arms of the same bridge from being turned on at the same time to cause a short circuit of the power supply, the turn-on of the lower arm must be later than the turn-off of the upper arm. Therefore, equation (12) can be obtained (Wang et al., 2014).

$$\Delta t \geq r \times \left[\left(t_{d(off)} + t_f - t_{d(on)} \right) + \left(t_{pdd\_max} - t_{pdd\_min} \right) \right] \tag{12}$$

In the formula:

r safety margin, usually between 1.2 and 1.5

t_{pdd_max} maximum transmission delay time

t_{pdd_min} minimum transmission delay time.

Taking Infineon's IKCM30F60GA as an example, the parameters of its switching time are as follows:

- $t_{d(off)}$ = 500 s
- t_f = 400 ns
- $t_{d(on)}$ = 555 ns
- t_{pdd_max} = 900 ns
- t_{pdd_min} = 600 ns.

From equation (9) we can get $\Delta t \geq 967.5$ ns. Considering a certain safety margin, we choose $\Delta t \geq 1$ μs.

Figure 5 Definition of IGBT switching time

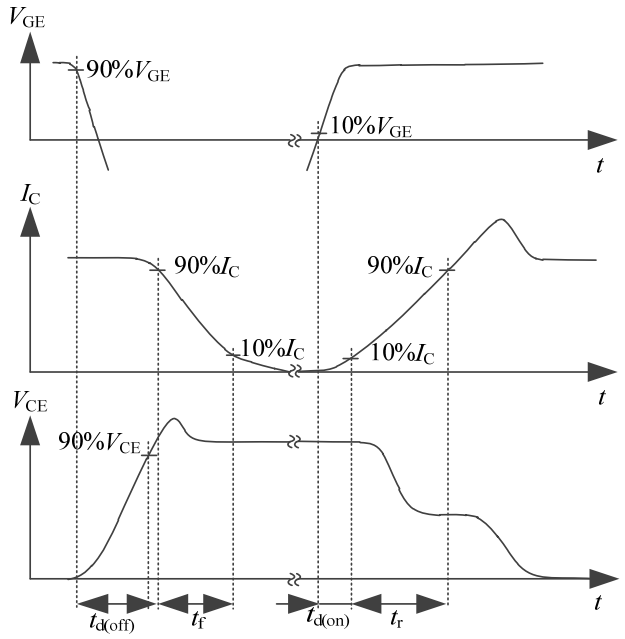

3.2 Equivalent dead time

It can be obtained from Section 3.1 that the turn-on and turn-off of the IGBT is not an ideal PWM rectangular pulse, but a rising and falling process. In order to make the simulation results more reliable, the following analysis is made:

The graphs enclosed by the solid lines in Figures 6(a) and 6(b) show the comparison of the simulated and actual waveforms of the PWM wave when the dead time is inserted.

For the convenience of calculation, the V_{CE} amplitude of the IGBT is set to 1, and the inserted dead time Δt is set to 2 μs. It can be seen from Figure 6(a) that in the simulated PWM pulse, V_{CE} rises from 0 to 1 instantaneously after the dead time Δt. However, V_{CE} does not fall instantaneously like the ideal falling edge. Before the ideal falling edge, V_{CE} drops from 1 to 0 along the hypotenuse of ②, and the endpoint coincides with the ideal falling edge. The falling time t_{fx} is 500 ns (measured value). It can be seen from Figure 6(b) that in the actual PWM wave pulse, because of the junction capacitance, V_{CE} rises from 0 to 1 along an arc after the dead time Δt, and the rise time t_r is 1,400 ns (measured value). Similarly, when the pulse falls, after the ideal falling edge, V_{CE} falls from 1 to 0 along an arc, and the falling start point coincides with the ideal falling edge. The falling time t_f is 100 ns (measured value).

Figure 6 Dead time setting comparison

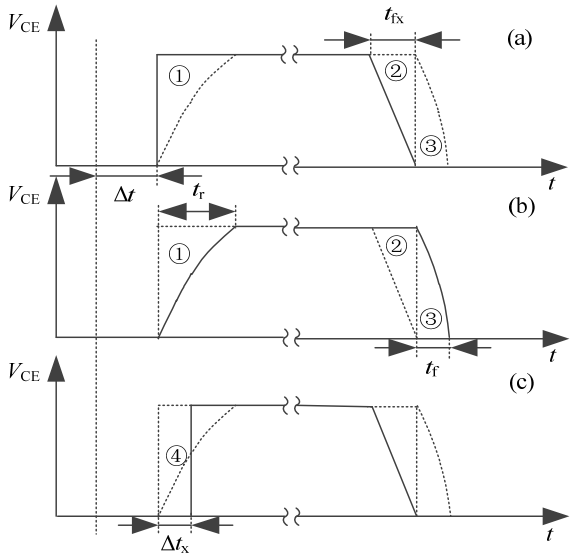

In sampling control theory, the impulse equivalence principle means when narrow pulses of equal impulse but different shapes pass through the inertial link, their effects are the same. According to the impulse equivalence principle, comparing Figures 6(a) and 6(b), it can be seen that in a pulse range, the simulated pulse is the area of graphics ① more than the actual pulse, and the actual pulse is the area of ② + ③ more than the simulated pulse. By calculating the difference between the impulse area of graph ① and graph ② + ③, and then dividing by the amplitude of V_{CE}, the pulse width Δt_x of rectangular pulse ④ in Figure 6(c) can be obtained as 400 ns (calculated value).

In summary, the simulation dead time setting closer to the actual situation can be expressed as: DT = $\Delta t + \Delta t_x$. For example, if the dead time is set to 2 μs in the actual situation, then it is set to 2.4 μs in the simulation.

4 Piecewise linear Lagrangian interpolation algorithm for selecting optimal switching frequency

The relationship between THD, switching frequency and dead time is shown in Figure 7.

It can be seen that for different dead time, there is a trend that THD first decreases and then increases as the switching frequency increases, and the longer the dead time, the more obvious the trend. There is an optimal switching frequency for different dead time to minimise THD. Therefore, we proposed a piecewise linear Lagrangian

interpolation algorithm for selecting the optimal switching frequency. The basic parameters are shown in Table 1.

Figure 7 The relationship between THD, switching frequency and dead time (see online version for colours)

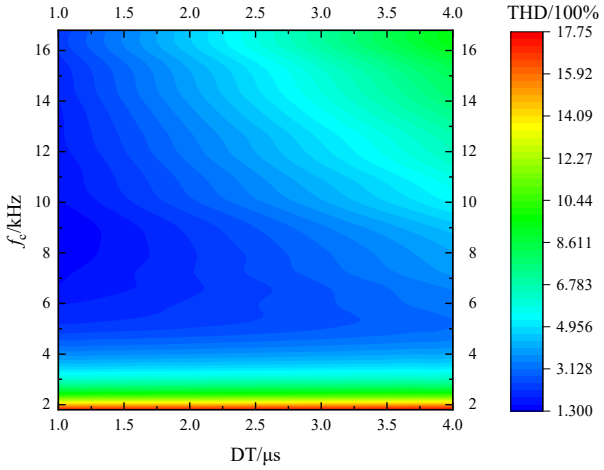

Table 1 Basic parameters

Parameters	*Values*
DC voltage V_{in}	240 V
Filter inductance L	5 mH
Filter capacitor C	10 μF
Load resistance R	16 Ω
Output power P	750 W
Dead time Δt	2 μs
Modulation degree M_r	0.8
Modulation wave frequency f_s	50 Hz

Take the dead time DT as 1~4 μs, and sample every 0.2 μs to analyse the change of THD when the switching frequency changes. The relationship between the optimal switching frequency and the dead time is shown in Figure 8.

Figure 8 The relationship between optimal switching frequency and dead time (see online version for colours)

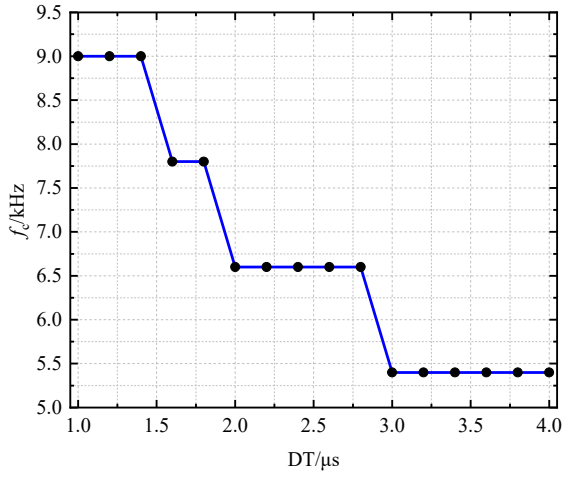

Let $L_n(x)$ be a straight line passing through two points $(DT_{n-1}, f_{c(n-1)})$, (DT_n, fc_n), then:

$$L_n(DT) = l_{n-1}(DT) f_{c(n-1)} + l_n(DT) f_{cn} \tag{13}$$

In the formula:

$$l_{n-1} = \frac{DT - DT_n}{DT_{n-1} - DT_n}, l_n = \frac{DT - DT_{n-1}}{DT_n - DT_{n-1}}.$$

Here $l_n(DT_{n-1})$ and l_n can be regarded as interpolation polynomials, which satisfy the conditions $l_{n-1}(DT_{n-1}) = 1$, $l_{n-1}(DT_n) = 0$, $l_n(DT_{n-1}) = 0$, $l_n(DT_n) = 1$.

Finally, the piecewise linear Lagrangian interpolation model of the optimal switching frequency f_c and THD can be obtained as shown in equation (14). Therefore, the optimal switching frequency f_c can be uniquely determined by substituting the dead time DT:

$$f_c = \begin{cases} L_1(DT) = 9000,\ DT \in [1, 1.4] \\ L_2(DT) = -6000DT + 17400,\ DT \in (1.4, 1.6] \\ L_3(DT) = 7800,\ DT \in (1.6, 1.8] \\ L_4(DT) = -6000DT + 18600,\ DT \in (1.8, 2] \\ L_5(DT) = 6600,\ DT \in (2, 2.8] \\ L_6(DT) = -6000DT + 23400,\ DT \in (2.8, 3] \\ L_7(DT) = 5400,\ DT \in (3, 4] \end{cases} \tag{14}$$

5 Experimental verification

According to the system parameters in Table 1, a three-phase four-wire SPWM inverter prototype system was built.

As shown in Figure 9, the system was controlled by TMS320F28335 produced by TI. The 62020H-150S programmable DC power supply from Chroma was selected, and the DC side voltage V_{in} was provided by two power supplies in series communication. V_{in} passes through a three-phase inverter bridge and LC filter, and outputs three-phase alternating current to supply power to the load. The negative terminals of the loads were connected to the midpoint of the two DC power supplies. The test system used Tektronix's TPS2014B oscilloscope and PA4000 power analyser.

Figure 9 Experimental prototype (see online version for colours)

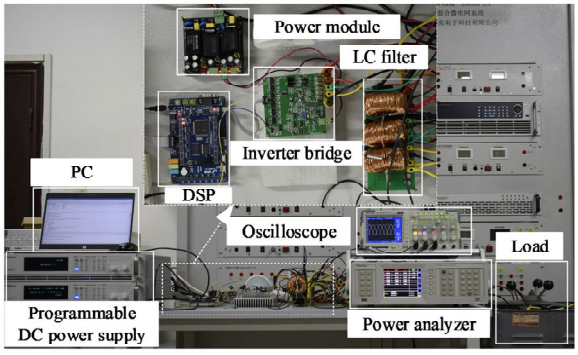

Figure 10 Experimental results (see online version for colours)

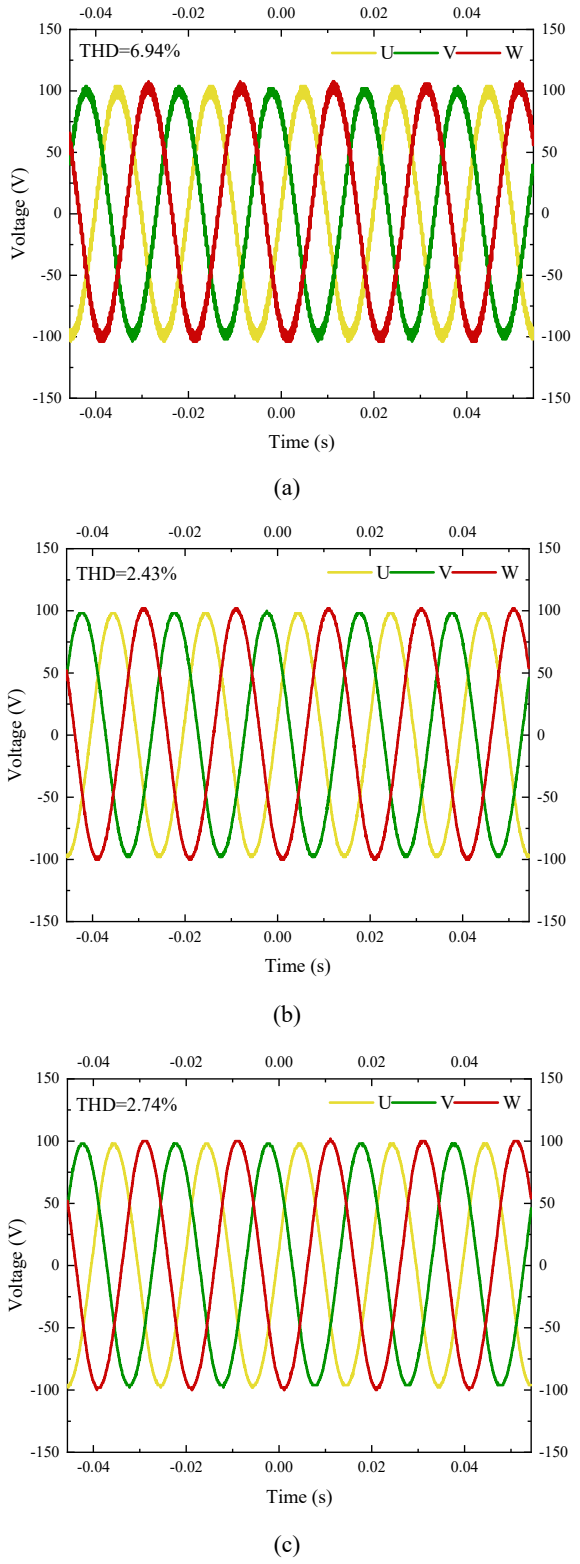

Set the switching frequency range 3.6 kHz~16.8 kHz. Observe the waveform of the output voltage, and perform FFT analysis on it. The experimental results are shown in Figure 10. Among them, Figure 10(a) is the situation when the switching frequency was set as 3.6 kHz. It can be seen that the output voltage waveform distortion is obvious. The THD was 6.94%, the output voltage measured by the power analyser was 65.468 V, and the efficiency was 95.9%. Figure 10(b) shows the situation when the switching frequency was set to 9 kHz. It can be seen that the high-order harmonic content of the output voltage was decreased, and the low-order harmonic content was increased. The THD was 2.53%, the output voltage measured by the power analyser was 65.059 V, and the efficiency was 95.8%. Figure 10(c) shows the situation when the switching frequency was set as 16.8 kHz. Figure 10(c) shows the situation when the switching frequency was set as 16.8 kHz. It can be seen that the waveform was slightly distorted, and the THD was 2.74%. The output voltage measured by the power analyser was 64.545 V, and the efficiency was 94.7%.

The change of THD with the switching frequency is shown in Figure 11. The green diamond and curve are the simulation data and the fitted curve. It can be seen that the lowest point was around 6.6 kHz. The red circle and curve are the experimental data and the fitted curve, the lowest point is around 9 kHz.

Due to the experimental environment and the electromagnetic interference of the test equipment, the THD fluctuates in a small range, but the trend of THD with the switching frequency is not changed. In addition, since the switching loss increases with the increase of the switching frequency, the switching frequency selected by this scheme not only reduces the switching loss, but also improves the voltage utilisation rate under the premise of ensuring the lowest output THD.

Figure 11 Variation of THD along with switching frequency (see online version for colours)

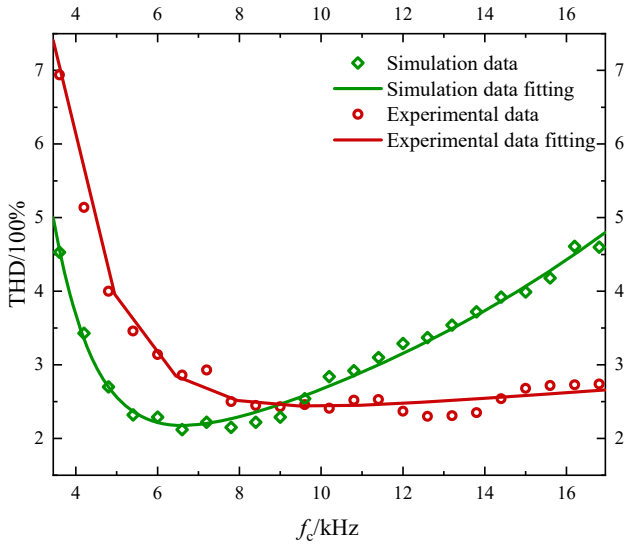

6 Conclusions

Taking the three-phase four-wire inverter as the research object, in this paper, a method to select the switching frequency based on the minimum THD as was proposed. It is generally believed that increasing the switching frequency is one of the means to reduce THD. However, through a lot of research work, this paper found that there is a switching

frequency point that minimises the output voltage THD when the dead time was considered. Considering the working process of the IGBT, and according to the principle of equivalence of impulse, a dead time setting rule closer to the actual situation was proposed. A piecewise linear Lagrangian interpolation algorithm was used to fit the calculation formula of the switching frequency. Finally, the effectiveness of the theoretical analysis was verified through experiments. Since the excessive increase of the switching frequency will cause unnecessary switching losses, this method not only optimises the THD, but also improves the utilisation of the DC side voltage. This paper had analysed three-phase four-wire off-grid inverter, and the conclusions obtained can be extended to the research of grid-connected inverters.

Acknowledgements

This work was supported in part by the National Natural Science Foundation of China (U1813201, 62073297, 61973157); National Key Research and Development Project of China (2020YFB1712403); Scientific and Technological Project in Henan Province of China (202102210097, 202102210135); Fundamental Research Foundation of Zhongyuan University of Technology (K2020TD005, K2019YY005).

Reference

Chitsazan, M.A. and Trzynadlowski, A.M. (2017) 'A new approach to LCL filter design for grid-connected PV sources', *American Journal of Electrical Power and Energy Systems*, Vol. 6, No. 4, pp.57–63.

Emami, S.A. and Banazadeh, A. (2013) 'Robustness investigation of the linear multi-variable control technique for power management of DFIG wind turbines', *Int. J. Advanced Mechatronic Systems*, Vol. 5, No. 1, pp.37–46.

Holmes, D.G. (1998) 'A general analytical method for determining the theoretical harmonic components of carrier based PWM strategies', *Conference Record of 1998 IEEE Industry Applications Conference, Thirty-Third IAS Annual Meeting*, Cat. no. 98CH36242, Vol. 2, pp.1207–1214.

Hu, Z.C., Li, Z., Wang, H. and Zhang, J.W. (2015) 'Study on optimal design of switching frequency for three-level converter', *Chinese Journal of Power Sources*, Vol. 39, No. 10, pp.2288–2290, 2315.

Huang, Z.L., Zeng, J. and Feng, L. (2018) 'Dead-time compensation strategy of three level inverter based on FFT', *Electric Drive*, Vol. 50, No. 6, pp.41–47.

Jeong, S.G., Zeng, J. and Park, M.H. (1991) 'The analysis and compensation of dead-time effects in PWM inverters', *IEEE Transactions on Industrial Electronics*, Vol. 38, No. 2, pp.108–114.

Ma, M.Y., Ling, F., Sun, Y.R., Li, F. and Zhang, X. (2020) 'Review of intelligent fault diagnosis methods for three-phase voltage-mode inverters', *Proceedings of the CSEE*, Vol. 40, No. 23, pp.7683–7699.

Ni, R.Z., Li, T., Chen, J. and Liu, Z.G. (2019) 'Research on a pulse dead zone compensation method', *Transactions of China Electrotechnical Society*, Vol. 34, No. S2, pp.553–559.

Song, C.H., Diao, N.Z., Xue, Z.W. Sun, X.R. and Guan, J.N. (2014) 'A novel lulti-carrier no-dead-zone SPWM', *Proceedings of the CSEE*, Vol. 34, No. 12, pp.1853–1863.

Song, L., Yang, Z.X., Yang, H.H. and Hou, S.Q. (2011) 'Experimental research on performance of vertical-axis three-hastate wind wheel', *Int. J. Advanced Mechatronic Systems*, Vol. 3, No. 5, pp.365–374.

Sukegawa, T., Kamiyama, K., Matsui, T. and Okuyama, T. (1988) 'Fully digital, vector-controlled PWM VSI-fed AC drives with an inverter dead-time compensation strategy', *Conference Record of the 1988 IEEE Industry Applications Society Annual Meeting*, Vol. 1, pp.463–469.

Sun, Z.J., Dong, T.H., Zhou, F., Zhang, X. and Wang, K.L. (2020) 'Influence of PWM switching frequency on rotor loss and temperature rise', *Micromotors*, Vol. 53, No. 2, pp.37–42.

Wang, B., Luo, Y.F., Liu, B.L. and Tang, Y. (2014) 'Analysis of dead time set for insulated gate bipolar transistor under different load conditions', *High Voltage Engineering*, Vol. 40, No. 11, pp.3584–3589.

Wang, D.F., Wang, M.Y., Shen, Y.L., Li, Q. and Xiu, L. (2020) 'Online feedback dead time compensation strategy for three-level T-type inverters', *IEEE Transactions on Industrial Electronics*, Vol. 67, No. 9, pp.7260–7268.

Wu, Z., Li, H., Zuo P. and Liu, W.Z. (2001) 'Analysis and restraint of harmonics for inverting power supplies using natural sampling SPWM', *Power System Technology*, Vol. 25, No. 4, pp.17–20.

Zhang, J.Y., Shu, J., Wang, H., Huang, L. and Ding, J.N. (2018) 'Dead-time compensation strategy based on current vector for three-level inverter', *Acta Energiae Solaris Sinica*, Vol. 39, No. 6, pp.1637–1645.

Zhou, Y., Fan, Q.L., Liu, J.C. and Lin, F. (2010) 'Simulation of voltage total harmonic distortion in inverter circuits', *Proceedings of the CSU-EPSA*, Vol. 22, No. 4, pp.100–102.